All-fiber multimode interference bandpass filter

Waleed S. Mohammed and Peter W. E. Smith

Department of Electrical and Computer Engineering, University of Toronto, Toronto, Ontario, Canada

Xijia Gu

Department of Electrical and Computer Engineering, Ryerson University, Toronto, Ontario, Canada

Received April 20, 2006; revised June 6, 2006; accepted June 17, 2006;
posted June 22, 2006 (Doc. ID 70154); published August 9, 2006

A novel design for an all-fiber bandpass filter based on a multimode interference reimaging phenomenon is presented. The filter has achieved low insertion loss with adequate bandwidth and isolation for coarse wavelength-division multiplexing. The filter can easily be made with any central wavelength that is compatible with the single-mode fiber used for its construction. The measured filter performance matches the theoretical predictions well. The filter can have broad applications in fiber-optic telecommunications, spectroscopy, and sensing. © 2006 Optical Society of America

OCIS codes: 060.2340, 060.4080.

Optical filters, and in particular all-fiber optical filters, are key components used extensively in fiber-optic communications for wavelength-division multiplexing (WDM) and also in spectroscopy and fiber-optic sensing. There are two types of fiber-based filter available commercially, fiber Bragg grating (FBG) filters and long-period grating (LPG) filters written in the core of a single-mode fiber (SMF).[1–3] Despite the success of FBGs in WDM technology, FBG filters are band rejection filters that need a relatively expensive circulator to be used in transmission. LPG filters can be reconfigured into a bandpass filter using two LPGs in series to couple resonant light from the fiber core into the cladding and then back into the core. The fiber core between the LPGs is blocked to eliminate nonresonant light.[4] The device has a large insertion loss of 2 dB and is relatively long. A simple fiber-based bandpass filter is still a subject of research.

In 2004, Mohammed *et al.*[5] reported a fiber-based wavelength-tunable condensing lens that consists of a SMF and a segment of multimode fiber (MMF).[5] This device can shift the axial focus position by tuning the input wavelength. A linear relationship between the input wavelength and the axial focus position was confirmed by experiments. A self-imaging phenomenon and its applications on multimode interference couplers was described by Soldano and Pennings using guided mode propagation theory.[6] A high-performance multimode interference filter was also proposed by Li *et al.* for 1.3 and 1.5 μm regions.[7] Nevertheless, those two papers described self-imaging for slab waveguides only, not for optical fiber. Selvas *et al.* reported a wavelength-tunable fiber laser that achieved tenability by changing the distance between the multimode fiber and a mirror.[8] The filtering aspects of the device, such as the peak transmission, bandwidth, and isolation, were not investigated.

Based on self-imaging theory, we predict that, if the core of another piece of SMF is spliced to the end of the MMF, this SMF–MMF–SMF combination should act as a bandpass filter. In this Letter, we report a fixed-wavelength bandpass filter based on multimode interference and reimaging. We investigated various factors such as MMF length and geometries of the SMF and MMF that affect the filter center wavelength, bandwidth, and isolation. We designed and fabricated a filter that achieved an insertion loss of 0.4 dB, a −3 dB bandwidth of 12 nm, and an isolation of 13 dB outside of ±25 nm from the central wavelengths over a 100 nm wavelength span. An excellent match was found between theoretically calculated spectra and the experimentally measured ones.

The filter proposed and investigated in this Letter is formed by splicing a segment of step-index MMF between two standard SMFs as illustrated schematically in Fig. 1. The detailed theory describing the multimode interference and reimaging phenomenon is presented in Ref. 5. The operating principles of the MMF bandpass filter can be briefly described as follows.

The light propagating along the input SMF enters the MMF with an approximate Gaussian-shaped field distribution that serves as the input field for the MMF segment. The input field excites a number of guided modes in the MMF as it propagates along the MMF. For a large MMF core radius the input field can be represented by a finite summation over the guided modes only, as increasing the MMF core size increases the number of guided modes and hence increases the confinement and minimizes the power in the cladding modes. Under these circumstances and using a linear polarization approximation, the field distribution at the end of the MMF segment of length z, can be written as[5]

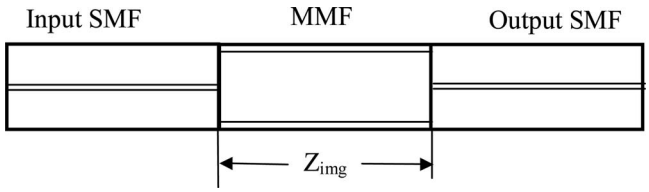

Fig. 1. Schematic diagram of an all-fiber multimode interference bandpass filter.

0146-9592/06/172547-3/$15.00

$$E_{\mathrm{MMF}}(r,\theta)=\sum_{j=0}^{M} a_j \psi_j(r,\theta)\exp(i\beta_j z), \tag{1}$$

where ψ_j and a_j are the jth mode electric field amplitude and the field expansion coefficient, respectively. The constant M is the total number of guided modes inside the MMF. For on-axis coupling, the number of modes is reduced to the number of radially symmetric modes.[5] The field expansion coefficients in Eq. (1) can be calculated from the following cross-correlation formula:

$$a_j=\frac{\int_{\theta=0}^{2\pi}\int_{r=0}^{\infty} E_s(r,\theta)\times\psi_j(r,\theta)^{*} r\,\mathrm{d}r\,\mathrm{d}\theta}{P_j},$$

$$P_j=\int_{\theta=0}^{2\pi}\int_{r=0}^{\infty}|\psi_j(r,\theta)|^2 r\,\mathrm{d}r\,\mathrm{d}\theta. \tag{2}$$

In Eq. (2), E_s is the field distribution of the SMF fundamental mode. The power coupling efficiency to the second SMF is calculated through the overlap integral between E_{MMF} and the second SMF fundamental mode. Using two identical SMFs, the total coupling efficiency can be written as[9]

$$\eta=\sum_{j=0}^{M-1}\sum_{h=0}^{M-1}\tilde{a}_j^2\tilde{a}_h^{*2}\exp[i(\beta_j-\beta_h)z], \tag{3}$$

where the modified expansion coefficient, $\tilde{a}_j$, is defined as

$$\tilde{a}_j=a_j\sqrt{P_j/P_s},\qquad P_s=\int_{\theta=0}^{2\pi}\int_{r=0}^{\infty}|E_s(r,\theta)|^2 r\,\mathrm{d}r\,\mathrm{d}\theta, \tag{4}$$

where P_s is the source power.

The coupling coefficient will reach a peak when the length of the MMF segment is selected so that the field distribution at the end of the MMF is an image of the input field. That length is referred to as the reimaging distance.[9] At this location the argument of the exponential term in Eq. (3) becomes an integer multiple of 2π, and hence the coupling efficiency is maximized. This condition is highly wavelength dependent. Deviation from this condition causes the coupling efficiency to drop. Thus it is expected that this SMF–MMF–SMF configuration will act as a wavelength filter. The transmission spectrum calculated using Eq. (3), shown in Fig. 2, confirms this prediction. In these calculations, the MMF refractive index is set to 1.443 with an air cladding, a 124 μm core diameter, and a 57.713 mm segment length.

In our experiments, we used a filter made with a single-mode fiber with a numerical aperture of 0.11 for the input and output SMFs and a section of Corning's 125 μm diameter no-core fiber for the MMF. A broadband LED was used as a light source, and the spectrum was measured with an optical spectrum analyzer (Ando Corp., Model AQ6317). The transmission spectrum of a filter with a 57.7 mm long MMF segment is shown in Fig. 2. Its peak coupling coefficient of 90.3% matches the simulation value very well, and its full width at half-maximum (FWHM) bandwidth of 13 nm is about 2 nm broader than the simulation FWHM of 11 nm. One possible explanation is that experimentally there may be some excitation of higher-order azimuthal modes due to a slight misalignment between the SMF and MMF segments while splicing. The simulation includes only radially symmetric modes.

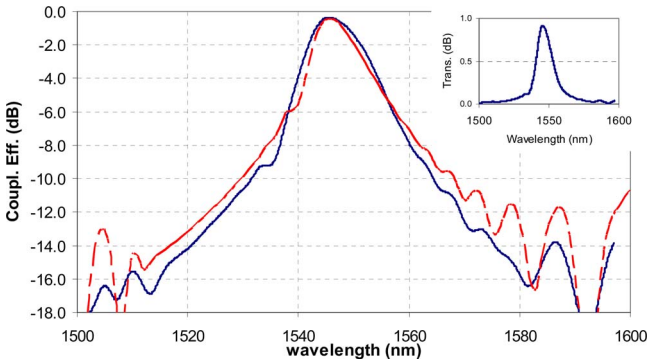

Fig. 2. (Color online) Comparison between the simulated spectrum (dashed curve) and the experimentally measured spectrum (solid curve) for a multimode interference-based bandpass filter. The inset shows the transmission spectrum plotted on a linear scale.

Isolation is an important parameter in a WDM system that measures how well different channels are separated. Figure 2 shows that the difference between the peak transmission at 1546 nm and the transmission outside of the ±25 nm range from the central wavelengths is over 13 dB in a wavelength span of about 100 nm. So if this filter is used in a WDM system where another channel is 25 nm from this channel, over 13 dB of isolation can be achieved. However, other transmission peaks with much lower coupling coefficients due to multimode interference are also present outside of that 100 nm wavelength span. It was observed that isolation depends on the numerical aperture of the SMF used. If the numerical aperture of the SMF is 0.14, the isolation of the fiber will be reduced to about 10 dB in the same wavelength span. To increase peak coupling coefficient and isolation, the phase difference between the guided radial modes in MMF should equal to a multiple of 2π. As Fig. 3 shows, by proper selection of SMF and MMF parameters to minimize the residual phase difference, the isolation can be increased. A significant advantage of this filter is that the central wavelength can be adjusted easily by changing the MMF length or finely tuned by applying strain on the fiber. Simulation shows that for every millimeter of increase of MMF length, the filter central wavelength can be tuned by 26.6 nm as illustrated by Fig. 4(a). Experimentally, we measure a strain tuning rate of -1.92 pm/μ strain, as depicted in Fig. 4(b). These measurements are in good agreement with simulations that applied tensile stress on the MMF to increase its length. A Poisson ratio of 0.17 was used to compute the fiber diameter decrease with increasing tensile stress. The other parameters used in the

simulation were the same as those used in the simulation for the filter transmission spectrum.

The filter bandwidth can be controlled by changing the MMF core size. Figure 3 shows simulated filter spectra as a function of MMF core size. The bandwidth increases as the core size of the MMF decreases. A decrease in core size must be accompanied by a decrease in the MMF length to maintain the same filter center wavelength as shown in Fig. 3. This bandwidth control feature will be useful for designing broadband filters for spectral shaping applications, such as trimming the spectral shape of amplified spontaneous emission from a semiconductor optical amplifier source into a Gaussian shape for optical coherence tomography. The filter bandwidth can be increased further by selecting a smaller core size of the MMF fiber. It should also be noted that because of the reimaging properties of the MMF segment, a doubling of the length of this segment will provide a filter with the same central wavelength and approximately half the bandwidth.

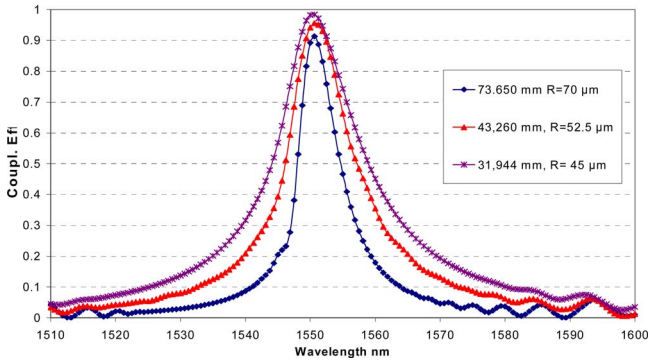

Fig. 3. (Color online) Filter bandwidth for different MMF core sizes. The numbers in the legend indicate the reimaging length and the radius of the MMF.

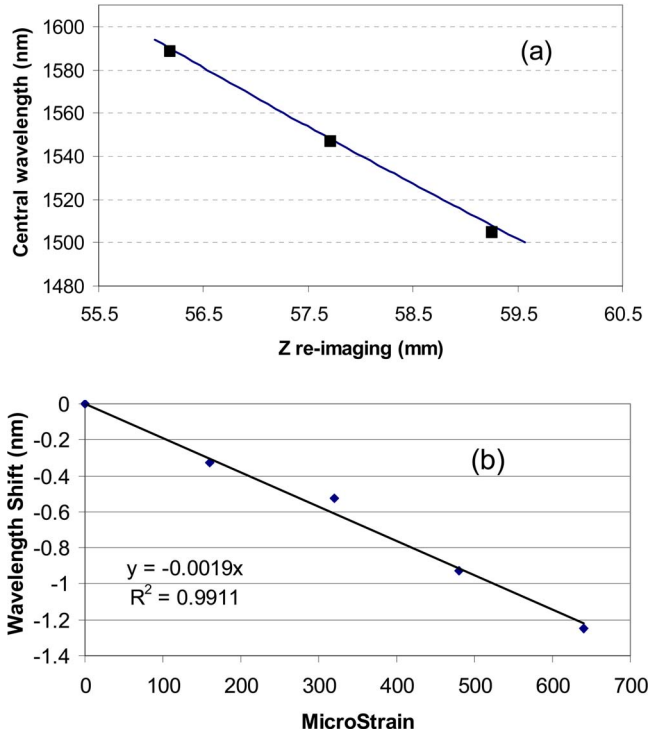

Fig. 4. (Color online) Filter central wavelength dependence on (a) MMF segment length and (b) strain, where the solid curve shows the simulation results and the filled squares are the experimentally measured data.

In conclusion, we have demonstrated a simple but highly functional bandpass filter based on multimode interference and reimaging. We investigated the relationships among the MMF segment length, the geometries of SMF and MMF, and the filter parameters such as center wavelength, bandwidth, and isolation. The simulation matched our experimental data very well. The filter exhibits a low insertion loss of 0.4 dB, a −3 dB bandwidth of 13 nm, and an isolation of 13 dB over a 100 nm wavelength span. The filter can also be packaged relatively easily since its length is about 6 cm. This type of filter can have many applications such as channel selection in coarse wavelength-division multiplexing spectroscopy, and fiber-optic sensing.

X. Gu's e-mail address is xgu@ee.ryerson.ca.

References

1. K. O. Hill, Y. Fujii, D. C. Johnson, and B. S. Kawasaki, Appl. Phys. Lett. **32**, 647 (1978).
2. G. Meltz, W. W. Morey, and W. H. Glenn, Opt. Lett. **14**, 823 (1991).
3. A. M. Vengsarkar, P. L. Lemaire, J. B. Judkins, V. Bhatia, T. Erdogan, and J. E. Sipe, J. Lightwave Technol. **14**, 58 (1996).
4. D. S. Starodubov, V. Grubsky, and J. Feiberg, IEEE Photon. Technol. Lett. **10**, 1590 (1998).
5. W. S. Mohammed, A. Mehta, and E. G. Johnson, J. Lightwave Technol. **22**, 469 (2004).
6. L. B. Soldano and E. C. M. Pennings, J. Lightwave Technol. **13**, 615 (1995).
7. B. Li, S. Chua, C. W. Leitz, and E. A. Fitzgerald, Opt. Eng.**41**, 723 (2002).
8. R. Selvas, I. Torres-Gomez, A. Martinez-Rios, J. A. Alvarez-Chavez, D. A. May-Arrioja, P. LiKamWa, A. Mehta, and E. G. Johnson, Opt. Express **13**, 9439 (2005).
9. W. S. Mohammed, X. Gu, J. Meier, and P. W. E. Smith, "Use of multimode interference in a multimode fiber segment to maximize on-axis coupling to radially symmetric specialty fibers" (submitted to Appl. Opt.)